Rhizosphere 33 (2025) 101024

Contents lists available at ScienceDirect

Rhizosphere

journal homepage: www.elsevier.com/locate/rhisph

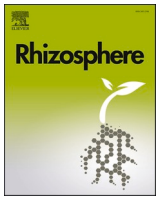

Plant-microbial interplay for organic nitrogen mediated by functional specificity of root compartments

Guoting Shen [a,*], Andrey Guber [b], Sajedeh Khosrozadeh [c], Negar Ghaderi [a], Alexandra Kravchenko [b], Evgenia Blagodatskaya [a]

[a] Department of Soil Ecology, Helmholtz-Centre for Environmental Research – UFZ, Halle (Saale), Germany
[b] Department of Plant, Soil, and Microbial Sciences, Michigan State University, East Lansing, MI, USA
[c] Department of Soil Science, College of Agriculture, Isfahan University of Technology, Isfahan, Iran

ARTICLE INFO

Keywords:
Amino-N
Leucine aminopeptidase
Maize (*Zea mays* L.)
Root parts
Rhizosphere
Time-lapse zymography

ABSTRACT

The organic form of nitrogen (N) is a critical intermediate in mutualistic and competitive root-microbial interactions, mediated by extracellular enzymes. Visualization of the hotspots of organic N and proteolytic activity might be valuable for revealing root functional specificity in N acquisition and transformation at the level of individual roots and compartments. For the first time, we used time-lapse amino-mapping and zymography to co-localize and map the spatial distribution of amino-N and leucine aminopeptidase (LAP) activity in the soil and different root parts of maize (*Zea mays* L.). Amino-N distribution was mainly associated with seminal roots and root tips, where it overlapped with LAP activity hotspots. In the lateral roots and bulk soil, however, LAP activity was decoupled from amino-N. Distinct functional traits revealed themselves as the highest amino-N content and LAP activity in seminal root tips and as the largest relative extent of the rhizosphere in lateral root tips. Co-localized amino-N and LAP activities highlighted different nutrient acquisition strategies mediated by root-microbe interactions, depending on the root compartment. Seminal roots and their tips appeared to adopt mutualistic strategies, potentially attracting root-associated microorganisms through releasing oligo- and polypeptides. In contrast, lateral roots, with amino-N detected only at their tips, demonstrated stronger N competition, relying on the enzyme activity of the rhizosphere microbial community for N acquisition. These insights emphasized the role of root functional specialization in shaping plant-microbe interactions, offering pathways to enhance nutrient use efficiency.

1. Introduction

Nitrogen (N) is an essential element for plant growth and a major limiting nutrient for primary production, strongly influencing transformation of organic residues in soil (Vitousek et al., 2002). As mineral forms of N are quickly taken up by plants and microorganisms, available N mainly occurs in the soil in the form of organic polymers, like polypeptides (Geisseler et al., 2010; Kuzyakov and Xu, 2013). These large organic molecules are inaccessible to plants and must first be broken down into simple compounds such as oligopeptides and amino acids, comprising approximately 6–31% of the water-soluble rhizodeposition in different plant species (Wichern et al., 2008). Hydrolysis of polypeptides is mediated by extracellular proteases (Greenfield et al., 2020), like leucine aminopeptidase (LAP) and tyrosine aminopeptidase, releasing amino acids such as leucine and other hydrophobic molecules (Sinsabaugh et al., 2008; Jian et al., 2016).

The concentration gradients of amino acids along the root axis, with higher levels nears root tips, reflect the specific functional traits and N acquisition strategies of roots (Pausch and Kuzyakov, 2011; Holz et al., 2018). For example, seminal roots are crucial role in the initial establishment of plants by facilitating the exploration of nutrients and water in the soil (Rogers and Benfey, 2015). Increasing the number of seminal roots has been reported to enhance N acquisition in low-N soils (Perkins and Lynch, 2021). The lateral roots exhibit a superior ability to forage for nitrate, which is highly soluble and prone to leaching into deeper soil layers (Postma et al., 2014; Zhan and Lynch, 2015; Yu et al., 2016). Root tips, unlike mature root regions, release organic compounds that selectively promote and modulate the populations of specific microorganisms (Hartmann et al., 2009; Amicucci et al., 2019), with differences in microbial community assembly and functions observed between mature

* Corresponding author. Department of Soil Ecology, Helmholtz-Centre for Environmental Research – UFZ, Theodor-Lieser-Str. 4, Halle (Saale), 06120, Germany.
E-mail address: guoting.shen@ufz.de (G. Shen).

https://doi.org/10.1016/j.rhisph.2025.101024
Received 1 October 2024; Received in revised form 19 December 2024; Accepted 6 February 2025
Available online 7 February 2025

lateral roots and root tips in maize (Rüger et al., 2021). Such functional differences, which suggest that amino-N spatial distribution may vary along roots and between root parts, need to be demonstrated experimentally.

Amino-N is a significant component of organic N sources in soil (Sinsabaugh and Follstad Shah, 2011; Geisseler and Horwath, 2014; Hill et al., 2019). Its content is closely associated with LAP activity, as amino-N can act as either a target substrate for enzyme or a product of extracellular enzyme activity (Matsui et al., 2006; Sinsabaugh et al., 2008). The localization of amino-N and LAP can be used to identify following scenarios (Fig. S1). Scenario 1: There is a positive correlation between amino-N and LAP activity. This can occur, e.g., under balanced input and decomposition of polymeric substrate released by the roots. There are two scenarios to consider when amino-N negatively correlates with LAP activity. Scenario 2: Increase in amino-N results in decrease in LAP activity. This is possible if soil microorganisms are not N-limited, e.g., after input of mineral N. Scenario 3: Decrease in amino-N results in increase in LAP. This indicates strong N limitation, low input of substrate and fast uptake of products, e.g., amino acids. Therefore, the colocalization of amino-N and LAP activity can help to reveal whether N limitation and the process of N transformation are specific to various root compartments. However, the spatial co-localization of enzymatic activity and N content at the soil-root interface remains poorly understood largely due to insufficiently developed methodology estimating the gradients of amino-N concentration within the rhizosphere.

The rhizosphere extent, the most interactive zone between roots and soil, is more sensitive to changes in N conditions than enzymatic activity rates (Hao et al., 2022). Traditional methods for estimating rhizosphere extent often use global thresholding applied to zymography images. These approaches rely on histograms of reaction rates across entire images to separate areas of high activity from low-activity zones, such as selecting the top 25% of activity values (Ma et al., 2017; Heitkötter and Marschner, 2018), or using the mean plus standard deviation to define thresholds for activity zones (Bilyera et al., 2020; Khosrozadeh et al., 2022). However, the high heterogeneity of soil and rhizosphere conditions makes global thresholding prone to inaccuracies. Differences in activity distribution among hotspots and their size can cause global thresholds to deviate significantly from locally relevant thresholds, especially as the target area increases. Therefore, a local thresholding that accounts for variability within hotspots, may provide more accurate estimates.

The objectives of this study were to: (1) assess the applicability of local thresholds for defining the rhizosphere extent of developed parts of seminal and lateral roots, as well as the youngest parts of roots — their tips; (2) evaluate how different root parts influence the distribution of amino-N within the rhizosphere extent; and (3) explore the relationship between amino-N distribution and LAP activity involved in N acquisition across maize root parts. To address these objectives, we further refined and applied amino-mapping technique (Khosrozadeh et al., 2023) to detect amino-N. This technique was combined with time-lapse zymography (TLZ), which improves accuracy by addressing the non-linearity of signal development and minimizing diffusion losses (Guber et al., 2021). We hypothesized that: (1) the highest amino-N content and LAP activity will be localized at the root tips; and (2) given the positive association between root diameter and exudation rate in crops (Williams et al., 2022), we hypothesized higher amino-N content at the tips of seminal roots compared to lateral roots; (3) co-localized zones of active N transformation will be revealed through combined amino-mapping and LAP zymography.

2. Materials and methods

2.1. Soil properties

The soil used in this study was originally sampled from 0 to 50 cm depth of Haplic Phaeozem, Saxony-Anhalt, Germany. The soil texture was loam (33% sand, 48% silt, and 19% clay). The total C in the soil was 8.5 g kg^{-1}, total N was 0.8 g kg^{-1}, available P was 32.7 mg kg^{-1}, and K was 28.5 mg kg^{-1} of dry soil mass. The soil pH ($CaCl_2$) was 6.4 (Vetterlein et al., 2021). The soil was sieved to a 1 mm particle size and fertilized with 1/3 of the recommended fertilizers dose: 16.7 mg kg^{-1} N (NH_4NO_3), 16.7 mg kg^{-1} K (K_2SO_4), and 8.3 mg kg^{-1} $MgCl_2$ $6H_2O$ added to the soil in liquid form, and 13.3 mg kg^{-1} $CaHPO_4$ added as powder, followed by thorough mixing. Subsequently, the soil was air-dried for 2 days. Then, the soil was passed through a 1 mm sieve again for even distribution of the fertilizers before filling the rhizoboxes.

2.2. Plants growth in rhizoboxes

Six rhizoboxes (2.6 × 9 × 15 cm, width × length × height, Clickbox®) were filled with the soil to a bulk density of 1.26 g cm^{-3}, then maize seeds (*Zea mays* L.) were sown at a depth of 1 cm. Details regarding the processing and planting of seeds can be found in Ghaderi et al. (2022) and Khosrozadeh et al. (2022).

The rhizoboxes were placed in a growth chamber at an angle of 45° to promote root growth along the wall. During plant growth, the temperature was maintained at 22 °C during the day and 18 °C during the night, and distilled water was added to the rhizoboxes every day to compensate for evapotranspiration losses and maintain soil water content at 22% (v/v). After three weeks of plant growth, amino-mapping and zymography were performed to visualize the distribution of amino-N and leucine aminopeptidase activity in the rhizosphere.

2.3. Identification of root parts

Daylight images were used to identify different root parts and younger roots. Root tips represent the youngest root parts, while the segments located beyond the root tips correspond to developed regions (Vetterlein and Doussan, 2016). Since the root-soil surfaces for imaging are not entirely flat, some areas may not have as much contact with the membrane as others. Therefore, daylight images of the roots were combined with zymograms to identify whether root parts have good membrane attachment, and only areas displaying clear signals were selected for further analysis.

2.4. Co-localization of amino-N and LAP activity

The rhizoboxes for amino-mapping and zymography were split into two groups. In one group (three rhizoboxes), membranes were placed at different locations for amino-mapping and LAP zymography to minimize any potential interference between the two techniques. In the second group (another three rhizoboxes), both measurements were co-localized by placing the membranes with the corresponding substrates in the same position, and performing amino-mapping followed by LAP zymography (Fig. S1). This sequence was chosen based on tests using membranes saturated with borate buffer alone as negative control, which confirmed minimal residual fluorescence after amino-mapping (Fig. S2). Similarly, residual fluorescence was tested using membranes saturated with TRIZMA buffer alone ($C_4H_{11}NO_3$·HCl with CAS number: 1185-53-1, $C_4H_{11}NO_3$ with CAS number: 77-86-1, pH: 7.8) as negative control after LAP zymography.

A comparison between the two groups enabled to test the potential effect of amino-mapping on LAP activity. The results demonstrated that LAP activity was not affected by amino-mapping, because i) no residual fluorescence was detected after finalizing amino-mapping (Fig. S2), and ii) no significant differences were observed in the mean and maximum LAP activity of the membranes between the two groups (Table S1).

Each membrane set consisted of the 140 μm-thick cellulose nitrate membrane (0.2 μm pore size, 50 mm Ø, Whatman®, Cytiva 10401314) used for amino-mapping and the 100 μm-thick polyamide membrane (0.45 μm pore size, 5 × 3 cm, Tao Yuan, China) used for time-lapse zymography. The images of the membranes were collected using a

Nikon D3500 camera with an AF-P DX NIKKOR 18–55 mm f/3.5–5.6G VR lens (Nikon, Inc.). The camera settings were as follows: an aperture of f/6.3, an exposure time of 1/125 s, and an ISO of 25,600.

The same setup was used for time-lapse amino-mapping, LAP zymography, and their calibration. After opening the rhizoboxes from the root side, the membranes were soaked in the corresponding reagent or substrate and then placed on the soil-root surface for incubation under UV light. The surface was pre-wetted by spraying with water to ensure hydraulic contact with the membrane. To ensure the contact between membrane and soil-root interface and to prevent evaporation from the membrane, transparent glass was then placed over the membrane.

2.5. Amino-mapping

We applied a time-lapse amino-mapping approach, the method is based on the reaction of *o*-phthalaldehyde and β-mercaptoethanol (OPAME), which was previously used to measure the content of primary amines (Jones and Darrah, 1994; Jones et al., 2002; Khosrozadeh et al., 2023). The reaction produces fluorescent compounds that can be detected under UV light. First, to prepare the working reagent OPAME, we dissolved 50 mg of *o*-phthalaldehyde (OPA) in 5 ml of methanol, added 100 μl of β-mercapthoethanol (ME) to the OPA-methanol mixture, shook it under a fume hood, and added 200 ml of borate buffer. The buffer was prepared by dissolving 2.012 g of sodium tetraborate in deionized water, adjusting the pH to 9.5 using NaOH (1 M), and making the final volume up to 500 ml (0.02 M). The reagent was left overnight to reduce the background fluorescence.

The cellulose nitrate membrane was soaked in OPAME reagent and then placed on the soil-root surface for 10 min incubation. During membrane incubation, images were captured every 10 s for the first 2 min, and then every 30 s for the remaining 8 min. For calibration, we used standard L-leucine solutions at the range of concentrations: 0, 0.1, 0.5, 1, 3, 4, and 5 mM. Due to the fast reaction of the reagent with amino groups, 5 μl of each solution and 10 μl of OPAME reagent were directly applied to dry membranes. The membranes were photographed in dynamics (to consider diffusion) under UV light using the same settings as those used for the rhizobox samples. The calibration coefficient was calculated for the green channel of the calibration images as the slope between the mass of the applied standard solutions and the sum of the grayscale values within each calibration spot after subtracting the background image.

2.6. Leucine aminopeptidase (LAP) zymography

We used the TLZ approach to visualize and quantify LAP activity (Guber et al., 2021). TLZ relies on the fluorescent signal development in the membrane over time, allowing subtraction of background noises, residual fluorescence after amino-mapping, and auto fluorescence from the roots. For TLZ, the polyamide membranes were saturated in 10 mM L-leucine-7-amido-4-methylcoumarin hydrochloride solution (CAS number: 62480-44-8; fluorogenic substrates, Sigma Aldrich, Merck KGaA, Darmstadt, Germany), which is commonly used substrate for leucine aminopeptidase. After placing the substrate saturated membrane, a transparent glass was placed above the membrane to prevent evaporation. The LAP membranes were then incubated for 45 min (Guber et al., 2021). Dynamic images were captured immediately after the membrane application. During incubation, we captured one image per minute.

A time difference of one day between amino-mapping and LAP zymography was considered an optimal additional measure to reduce residual fluorescence and minimize the effects of continuous root growth. A standard calibration was prepared by adding 10 μl of 7-amino-4-methylcoumarin (AMC; CAS number: 26093-312-2) with a range of concentrations (0, 0.01, 0.02, 0.03, 0.04, and 0.05 mM) to a membrane. The Membranes were also photographed every minute for 45 min. The quantity of AMC per unit area was calculated, and a calibration line was used to convert the fluorescent signal from the zymograms into AMC concentrations.

2.7. Image processing

Zymography images were processed using ImageJ (version 1.51n) and MATLAB (R2021b) software following the TLZ protocol (Guber et al., 2021). Across six membranes tested, we identified three independent replicates displaying good membranes attachment for each root part and therefore, clear signals (Figs. S2 and S3). This limited number of replicates consistent with findings demonstrated that the fluorescence visualized by zymography represents only about 20% of the actual reaction area on the soil surface (Guber et al., 2018). For each replicated root part, including developed seminal and lateral roots and their tips, measurements were conducted along thirty transects (Fig. S4), with each transect extending from the root center out to the soil. It should be noted that no amino-N signals were detected on the lateral roots. Thus, the data for amino-N content originated from 30 transects × 3 root parts × 3 replicates, and the data for LAP activity originated from 30 transects × 4 root parts × 3 replicates.

For amino-mapping images, the green channel was used to calculate the amino-N content in membranes based on the calibration (Fig. S5) described by Khosrozadeh et al. (2023). For the leucine aminopeptidase, original zymography images were converted to 8-bit grayscale images to calculate LAP activity in membranes based on the calibration described by Guber et al. (2021). The first images taken at time zero, were subtracted from the whole sequence of images taken at 1–45 min to correct for the background, including root autofluorescence and residual fluorescence after amino-mapping. Random noise was removed from the images using the "Median 3D" filter. Substrate-specific calibrations were used to convert the grey values to L-leucine and AMC contents.

2.8. Rhizosphere extent determination

The rhizosphere extents of amino-N content and LAP activity were determined separately for each root part using two global thresholding approaches (mean + SD and mean + 2SD) and a local thresholding approach. For the global approaches, the thresholds were calculated as either mean + SD or as mean + 2SD of the activity histograms across the whole zymography area. For the local approach, the rhizosphere extent was determined individually for each root by identifying the distance from the root boundary where the first distance derivative of amino-N content and LAP activity became zero. This distance represents the point along the transect from the root surface where amino-N content and LAP activity no longer change with further increases in distance. We refer to this method as Local Zero Derivative Thresholding (LZDT).

The differences in intensity between neighboring pixels (gradients) measure contrast, with zero values indicating that neighboring pixels are similar in their properties. However, gradient methods are sensitive to noise, such as background interference or random fluctuations in the signal, so noise filtering is often applied to smooth the image. For this study, we used a polynomial regression model (Eq. (1)) to filter the data. This model provided the best fit to the cumulative values of amino-N content and LAP activity in the rhizosphere. Areas with zero contrast values, where amino-N content and LAP activity no longer change with distance, were considered part of the soil matrix. In contrast, areas with nonzero contrast values were classified as part of the rhizosphere. To minimize the effects of data oscillations, we first calculated the cumulative distribution of amino-N content and LAP activity along each transect. We then fitted these cumulative curves using a second-order polynomial regression (Fig. S6) as follows:

$$y = ax^2 + bx + c \quad (1)$$

here y represents the amino-N content or LAP activity, x is the distance

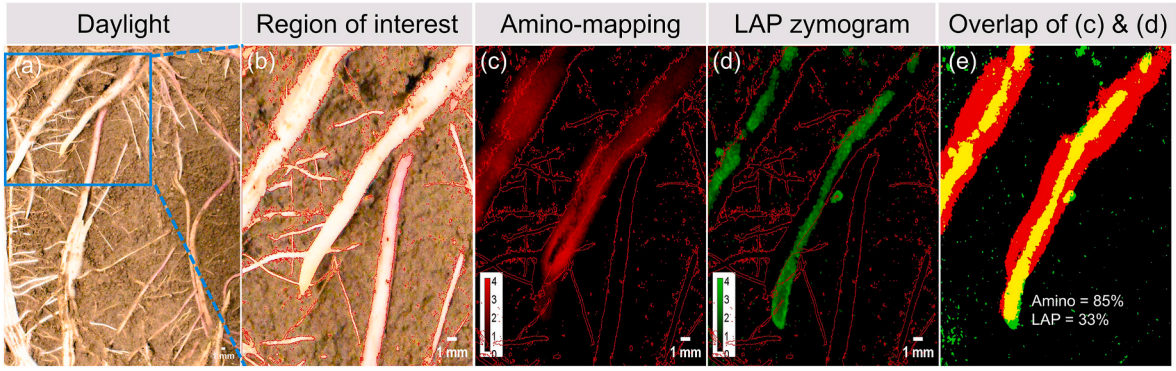

Fig. 1. Example of amino-N spatial distribution and co-localization of amino-N content and leucine aminopeptidase (LAP) activity in the young roots. (a, b) Daylight images with a big blue square indicating the region of interest. (b, c, d) Red lines highlight root boundaries. (c, d) Amino-N and LAP activity distribution is illustrated with a green bar indicating amino-N content (ng mm^{-2}) and LAP activity (pmol mm^{-2} min^{-1}). (e) The yellow overlap image represents the co-localization of roots (red) and amino-N (green). Co-localization analysis is presented via two coefficients: Amino (85% of the LAP area overlaps with amino-N), LAP (20% of the amino-N area overlaps with LAP).

from the root surface, and *a*, *b*, and *c* are polynomial coefficients. The rhizosphere extent was determined as the distance where the first derivative of Eq. (1) equaled zero, calculated by the formula:

$$x\,(0) = -\,0.5b/a \tag{2}$$

Comparison of the global (mean + SD and mean + 2SD) and local (LZDT) thresholds showed that the global thresholds considerably underestimated rhizosphere extents. This was because strong decreasing gradients were still observed beyond the mean + SD and mean + 2SD thresholds (Fig. 3d and 3e). In contrast, the local thresholds provided more accurate estimates of the rhizosphere extent. As a result, the local thresholds were used for further statistical analysis.

In addition to exploring the variation in amino-N content and LAP activity as a function of the distance from the root, we also separately analyzed them in three distinct areas of interest: the root surface, the rhizosphere in the immediate vicinity (0–0.2 mm) of the root, and the extended rhizosphere >0.2 mm distance from the root boundary to the end of the rhizosphere extent as determined by Eq. (2), for brevity referred further on as >0.2 mm rhizosphere. Based on our root hair length data (Table S2) and a previous study indicating that the influence of the root on protease activity was limited to a narrow zone <0.2 mm from the root surface (Greenfield et al., 2021), we surmise that the first 0.2 mm area from the root surface represents the most dense root hair zone. To facilitate comparisons among the root parts, in addition to total rhizosphere extent (Eq. (2)), we also determined the relative rhizosphere extent. That was obtained by normalizing the total rhizosphere extent as determined from Eq. (2) by dividing it by the corresponding root radius.

2.9. Statistical analysis

Co-localization analysis was performed to examine the overlap of amino-N and LAP activity zones with the root areas and with each other. Prior to statistical analysis, the root, amino-N and LAP activity images were juxtaposed using the Correlia registration plugin in ImageJ (Rohde et al., 2020). Then the co-localization was calculated separately for amino-N and LAP activity as:

$$\begin{aligned} Amino &= 100\%(S_{amino-N} \cap S_{LAP})/S_{LAP};\ LAP \\ &= 100\%(S_{amino-N} \cap S_{LAP})/S_{amino-N} \end{aligned} \tag{3}$$

where ∩ means intersection, $S_{amino-N}$ *and* S_{LAP} are amino-N and LAP active areas on images, respectively; *A* and *Z* are percentage of overlapped area of the total amino-N and LAP active areas, respectively.

The average activities of different root parts across different ranges were analyzed using a linear mixed model approach implemented in the lme4-package (Bates et al., 2015) of R (v.4.2.3). The statistical model consisted of fixed effects of the root parts, the spatial position from the root, and their interactions. Two ways of including the spatial position effects were considered: 1) representing the spatial position as three distinct regions, i.e., root surface, 0–0.2 mm rhizosphere, and >0.2 mm rhizosphere, and 2) directly assessing the distances within 0–1 mm from the root. All models included (i) the random effects of the root part replicates, used as an error term for testing the root part effects, and (ii) the random effects of the spatial position within each replicate root part, used as an error term for testing the effects of the spatial positions and their interactions with the root parts. The assumptions of normality and homogeneity of variances were assessed using normal probability plots of the residuals and Levene's tests for equal variance. When the interactions between the studied factors were found to be statistically significant ($P < 0.05$), slicing of the interaction, aka simple effect *F*-tests, were conducted and, when significant ($P < 0.05$), followed by multiple comparisons among the mean values. Pearson correlation coefficients were calculated between the values of amino-N content and LAP activity separately in different areas using the "corrplot" package (Wei et al., 2017).

3. Results

Juxtaposition of the root images and amino-mapping images revealed that amino-N hotspots were mainly associated with young seminal roots and root tips (Fig. 1c and S3a''). Fluorescent signals related to amino-N were either non-existent or much weaker in mature seminal roots than in young roots (Fig. 1c and S3a''). Remarkably, amino-N hotspots were located at the tips of the lateral roots, and were absent in the developed sections of lateral roots (Fig. 2c). Based on this observation, we recommend placing membranes on root tips and newly-developed roots to effectively identify hotspots of amino-N distribution. The concentration of amino-N in bulk soil was very low and almost negligible. The amino-N content was 7–15, 60–142, 10–25 times higher on seminal root tips, developed seminal roots, and lateral root tips, respectively, than in the corresponding rhizosphere soil. Similarly, LAP activity was respectively, 6–14, 8–18, and 4–8 times higher on seminal root tips, lateral root tips, and developed roots than in the rhizosphere soil (Table S3).

The amino-N content in the same root part was the highest at the root surface and decreased gradually with increasing distance from the roots (Figs. 3a, 3b, and 4). The differences in amino-N content between root compartments were only found on the root surface, with seminal root tips having a 23% higher amino-N content than that of mature seminal roots and lateral root tips (Fig. 4a, 4b, and 4c). There were no significant differences in the rhizosphere extent of amino-N content among the different root parts (Fig. S7). Given that the root diameter varied in

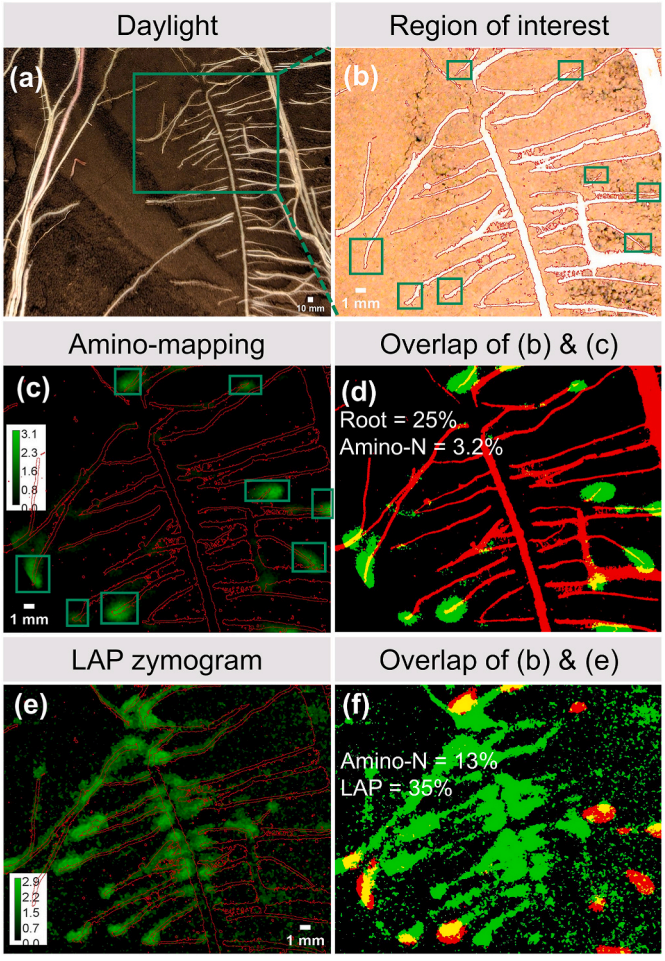

Fig. 2. Example of amino-N spatial distribution and co-localization of amino-N content and leucine aminopeptidase (LAP) activity in lateral roots. (a) Daylight image of the soil-root surface, with a green square indicating the region of interest: lateral roots. (b) Red lines highlight root boundaries, and small green squares indicate the lateral root tips position. (c) Amino-N distribution is illustrated with a green bar indicating the amino-N content (ng mm^{-2}). (d) The yellow overlap image represents the co-localization of the roots (red) and amino-N (green). Co-localization analysis is presented via two coefficients: Root (25% of the amino-N area overlaps with the roots) and Amino-N (3.2% of the root area overlaps with amino-N). (e) The distribution of LAP activity, with green bar indicating LAP activity (pmol mm^{-2} min^{-1}). (f) The overlap image of amino-N (red) and LAP activity (green) is shown in yellow. Amino-N (13% of the LAP area overlaps with amino-N) and LAP (35% of the amino-N area overlaps with LAP).

different root types and segments, the relative rhizosphere extent was standardized by the root radius. As a result, the relative rhizosphere extent of the lateral root tips was 2.9 and 3.5 times greater than that of the seminal roots and seminal root tips, respectively (Fig. 3c).

In contrast to amino-N, LAP activity was detected in both maize roots and the surrounding root-free soil (Figs. 2e and 5c). The level of LAP activity in the seminal root tips was the highest in the 0–0.2 mm distance zone, in comparison to other zones (Fig. 4d, 4e, and 4f). The same pattern was observed at the root surface and at a distance of 0–0.2 mm from the root, with the highest levels of LAP activity occurring at the seminal root tips in comparison to other root parts (Fig. 4 and Fig. S8). The level of LAP activity at the root surface and at a distance of 0–0.2 mm from seminal root tips was 16–32, 14–33, and 20–42% greater than that observed at corresponding distances from seminal roots, lateral root tips, and lateral roots, respectively. The lateral roots demonstrated the lowest rhizosphere extent of LAP activity relative to the other root compartments (Table S4). Notably, the relative rhizosphere extent of LAP activity at the lateral root tips was 1.2–3.4-fold greater compared to the other tested root parts (Fig. 3f).

The amino-N content and LAP activity hotspots were predominantly co-localized and showed a strong overlap in seminal roots (Fig. 5d) and root tips (Fig. 2f). The amino-N content and LAP activity were significantly positively correlated with each other on the root surface and rhizosphere areas across different root parts (Table S5).

4. Discussion

4.1. Advantages of the LZDT method for rhizosphere extent estimation

As an alternative to the global thresholding, we suggested a local approach (LZDT) to estimate the rhizosphere extent, which is based on the zero first distance derivative of the activity along the transect drawn perpendicular to individual roots or their parts. LZDT identified the specific distance at which the activity did not further increase with the distance from the root surface. In comparison with the global thresholding which traditionally used either mean + SD or mean + 2SD of the activity histogram calculated for the whole rhizobox area (Bilyera et al., 2021; Khosrozadeh et al., 2022), LZDT was tailored to individual roots, making the results more reliable and representative of the actual conditions of heterogeneous soil/root interactions. The rhizosphere extent was strongly underestimated by the mean + SD or mean + 2SD approaches (Fig. 3d and e), while LZDT convincingly provided reliable values for both the LAP and amino-N assays. This approach was useful for unifying the differences in the spatial distribution of amino-N and LAP activity observed in our study. Our results suggest that the global thresholding is more suitable for identifying the “hotspots” than for estimating the rhizosphere extent, as it ignores local variability of enzymatic activity. Therefore, LZDT can be considered among other local thresholding approaches for rhizosphere extent estimation owing to its broad applicability in heterogeneous soil conditions.

4.2. Spatial distribution of amino-N content

We demonstrated that seminal root tips had the highest amino-N content on the root surface compared to developed parts of seminal roots and lateral root tips (Fig. 4a), in line with our first hypothesis. In general, the exudation rates are higher at root tips and lower at more mature root parts (Jones and Darrah, 1994). Root exudates, such as low molecular weight compounds (e.g. amino acids), can be passively released from the root into the rhizosphere by diffusion. Compounds with specific functions in nutrient mobilization, defense response or root signaling can be released by active transport (Lipson and Näsholm, 2001; Leduc and Rothstein, 2010; Neumann and Römheld, 2011). However, it is important to note that our approach could not differentiate whether the detected amino-N originated directly from the roots or from associated microbial activity. Additionally, we found higher amino-N content on the surface of seminal root tips than lateral root tips, which partially supported our second hypothesis. In comparison to their corresponding developed parts, root tips have higher amino-N content, likely due to more intensive exudation of N-enriched proteinaceous compounds (Yu et al., 2021) and lower proportion of cellulose and other recalcitrant cell wall materials, which are depleted in N content (Neumann and Römheld, 2011). Inhomogeneous distribution of amino-N may also indicate a strategy to mitigate N limitation during root growth. Nutrient availability and chemical signals in the rhizosphere contribute to the establishment of root part-specific microbial communities that influence plant-microbial interactions and nutrient cycling. Therefore, bacteria in the rhizosphere of young plants quickly metabolize labile substrates like simple amino acids, while bacteria associated with mature tissues tend to utilize more complex carbohydrates (Houlden et al., 2008; Li et al., 2014). Such a ‘specialization’ of root tips in amino-N production enables the most efficient use of nutrient

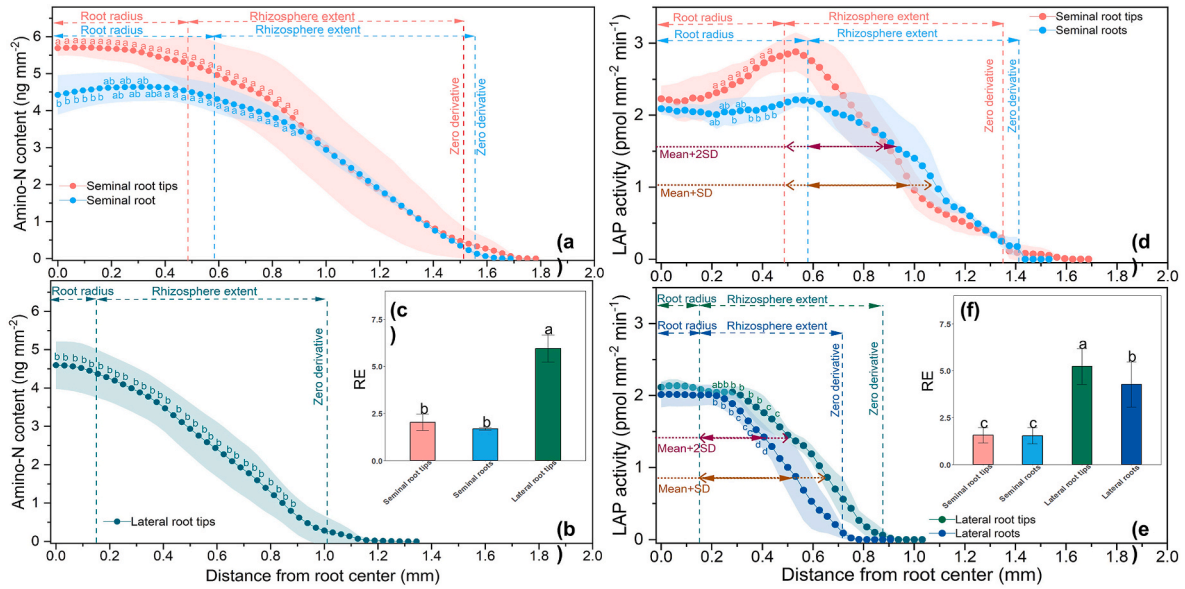

Fig. 3. Distribution of amino-N content and leucine aminopeptidase (LAP) from the root center to soil across various root parts (a, b, d, e) and relative rhizosphere extent (c, f). Vertical lines represent the position of the root boundary (left) and the threshold value for the rhizosphere extent (right). Different lowercase letters indicate significant differences among different root parts in amino-N contents or LAP activity at the same distance ($P < 0.05$). The relative rhizosphere extent (RE) was normalized by dividing the rhizosphere extent by the root radius (c). Different lowercase letters indicate significant differences ($P < 0.05$) in the relative rhizosphere extent among the seminal root tips, seminal roots, and lateral root tips. The shadowed areas indicate the standard deviation of the amino-N content and LAP activity. The plum red and earthy yellow dot lines indicate the rhizosphere extents that would be obtained by using mean + 2SD and mean + SD threshold approaches, respectively (d, e).

resources in plant-microbe interactions. Therefore, an attachment to root tips is considered as a key microbial trait that gives the microbes greatest access to available exudates and increases their proliferation along the root with limited energy expense (Dupuy and Silk, 2016). Besides, the higher absorptive capacity of lateral versus seminal roots, the secondary development of seminal roots resulting in larger diameter conduits and increased transport functions may also explain the lack of amino-N in lateral roots (McCormack et al., 2015). Remarkably, the amino-N content of developed seminal roots and root tips was higher in the 0–0.2 mm than in the >0.2 mm distance (Fig. 4b and c). As 0.2 mm distance corresponds to most dense part of the root hair zone of maize, root hair could play a "buffering" role by smoothing the sharp decline in amino-N content around the root.

4.3. Spatial distribution of leucine aminopeptidase activity

The highest LAP activity was observed in the seminal root tips at the root surface and in the 0–0.2 mm area. In >0.2 mm zone, the highest LAP activity was found on the lateral root tips, confirming the preferential localization of enzymatic hotspots around the root tips (Razavi et al., 2016). This can be attributed to the faster growth and higher metabolic activity of root tips compared with the other root parts, where fast-growing copiotrophic microbiome members dominate, with greater variability in population size and faster growth rates than oligotrophic bacteria (Fierer et al., 2007; Rüger et al., 2021). The buffering role of root hairs was also demonstrated for LAP activity, which did not differ significantly at the root surface and in the 0–0.2 mm area. Both amino-mapping and LAP activity zymography revealed the largest relative rhizosphere extent at the lateral root tips compared with the corresponding parts of the seminal roots and tips (Fig. 3c and f). Despite the larger relative rhizosphere extent for oxidative (Khosrozadeh et al., 2022) and hydrolytic enzymatic activities (Ma et al., 2018) reported for lateral roots compared with seminal roots in general, the functional differences between lateral root tips and lateral roots had not been clearly addressed before. Our study revealed the functional specificity of maize lateral root tips as large hotspots of amino-N and LAP activity relative to the root radius. Indeed, root systems with a higher density of root tips are characterized by high exudation rates owing to the reduced carbon costs of root construction and the large carbon investment in root exudation, which attracts mycorrhizal symbiosis (Darwent et al., 2003; Meier et al., 2020). Additionally, spatial distribution of LAP activity was different from amino-N which was not detected in root-free soil. This indirectly indicated that the LAP activity detected in the non-rooted soil may have a microbial origin, as in the absence of plant input, microorganisms likely produce LAP to acquire amino-N from the soil.

4.4. Co-localization of amino-N and leucine aminopeptidase activity

The different co-localization patterns of the seminal and lateral roots indicated that root-microbial interactions and mechanisms for nutrient acquisition varied in different root compartments (Fig. 6). Plants employ various strategies to attract beneficial microorganisms to their roots and actively deter the colonization of microbes that offer no advantages or pose a competitive threat to their growth environment (Hartman and Tringe, 2019). Amino-mapping coupled with LAP zymography revealed the co-localization of amino-N and LAP activity in the same regions of the seminal roots and root tips. This relationship was further confirmed by a positive correlation between the amino-N gradients and LAP activity in the rhizosphere (Table S5). Such a situation supported both our hypotheses and corresponded to the Scenario 1 (see Introduction), suggesting that polymeric substrates released by the roots attracted microorganisms and induced enzymes product to degrade these substrates. Seminal roots are known for their primary role in allocating seed-stored carbohydrates for root system establishment, efficiently acquiring soil resources and anchoring plants to the soil (Tai et al., 2016). Higher levels of amino-N in seminal roots, including polypeptides and proteinaceous compounds, provide a nutrient-rich environment and are chemically attractive to soil microbes, which has the potential to increase the number and activity of microorganisms (Bais et al., 2006). We assume, therefore, that amino-N in seminal roots served as substrates for aminopeptidases (like LAP) and induced high LAP activity. Small and readily available amino acids are released as products of

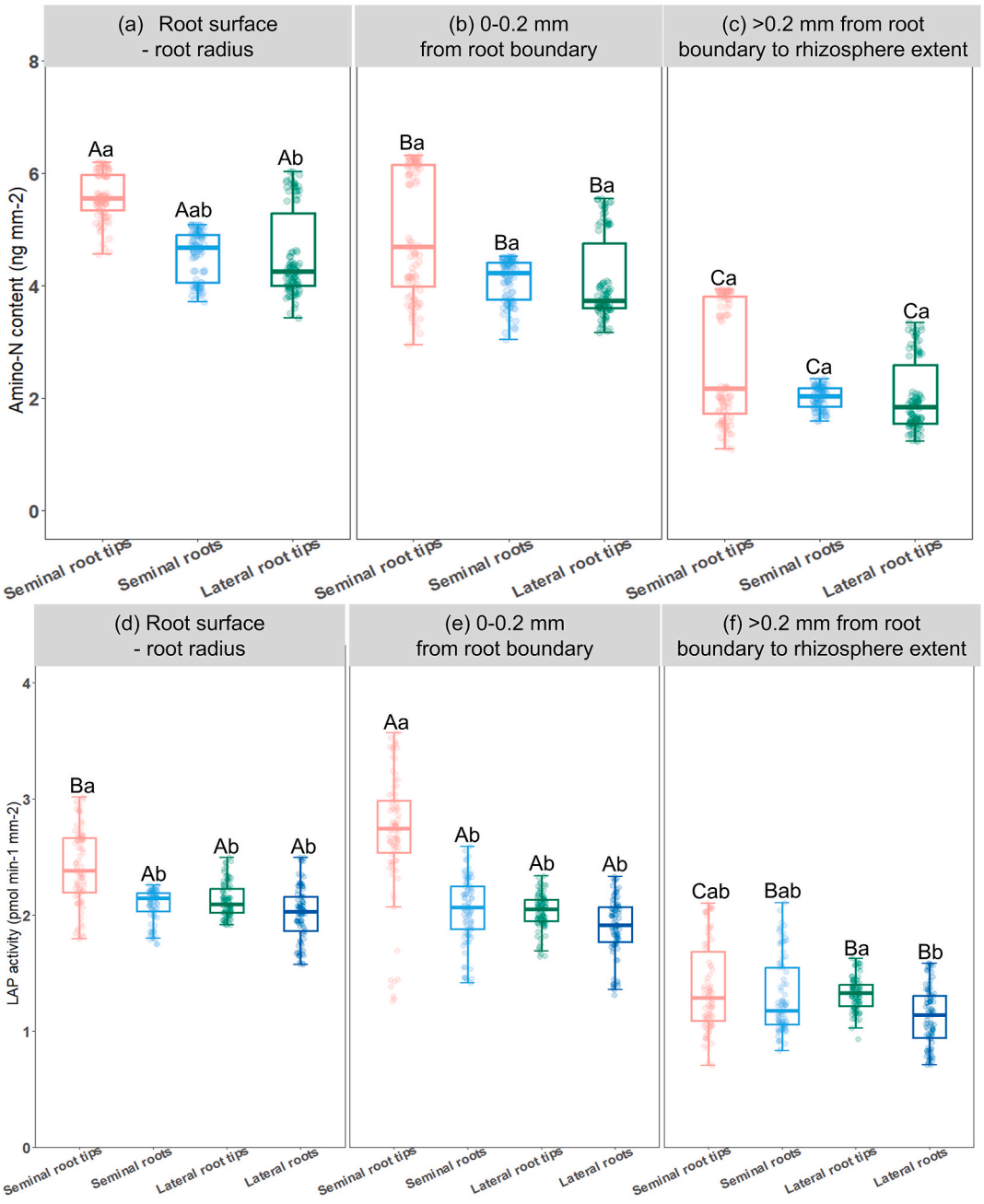

Fig. 4. The mean value of amino-N content and leucine aminopeptidase (LAP) activity in different root parts from different distances. The mean amino-N content (ng mm^{-2}) and LAP activity (pmol mm^{-2} min^{-1}) were calculated at the root surface (a, d), 0–0.2 mm distance from the root surface (b, e), and > 0.2 mm distance from the root surface to the rhizosphere extent (c, f) in seminal root tips, seminal roots, lateral root tips, and lateral roots. The data are presented as means for each part (n = 90), and the error bars indicate the standard deviations. Different lowercase letters indicate significant differences among different root parts from the same area ($P < 0.05$). Different capital letters indicate significant differences among different areas in the same root part ($P < 0.05$).

aminopeptidase activity, reducing microbial competition for N and forming a diverse rhizosphere community. The exudation of large amounts of monomeric amino acids by plants in excess of the products of aminopeptidases is unlikely in such a scenario, because it would result in reduction of LAP activity, corresponding to Scenario 2, which was not observed in our study.

Amino-N was coupled with LAP activity at the tips of lateral roots, while only LAP activity and no amino-N was detected on lateral roots (Figs. 2f and 5d). Lateral roots are mainly associated with the exploration for nutrients and water resources (Rogers and Benfey, 2015). As amino-N decreases along the lateral root axis, the initially random community assembly at the root tips is replaced by deterministic processes of community assembly through competition for nutrients and predation in the lateral root rhizosphere (Rüger et al., 2021). Lateral roots recruit microbes and shape the rhizosphere community by adjusting the exudation to alleviate the fierce competition in the rhizosphere, e.g., by releasing flavones to enrich the PGPB bacteria, such as Oxalobacteraceae with strong N acquisition ability (Yu et al., 2021). In line with Scenario 3, the LAP activity detected in the lateral roots supported that the microbial community played a significant role in coping with N competition. Essential LAP activity versus negligible amino-N content observed in bulk soil also corresponded well to a scenario 3. Since amino-N content in soil has been considered an indicator of plant N status (Canarini et al., 2019), the lower levels of amino-N

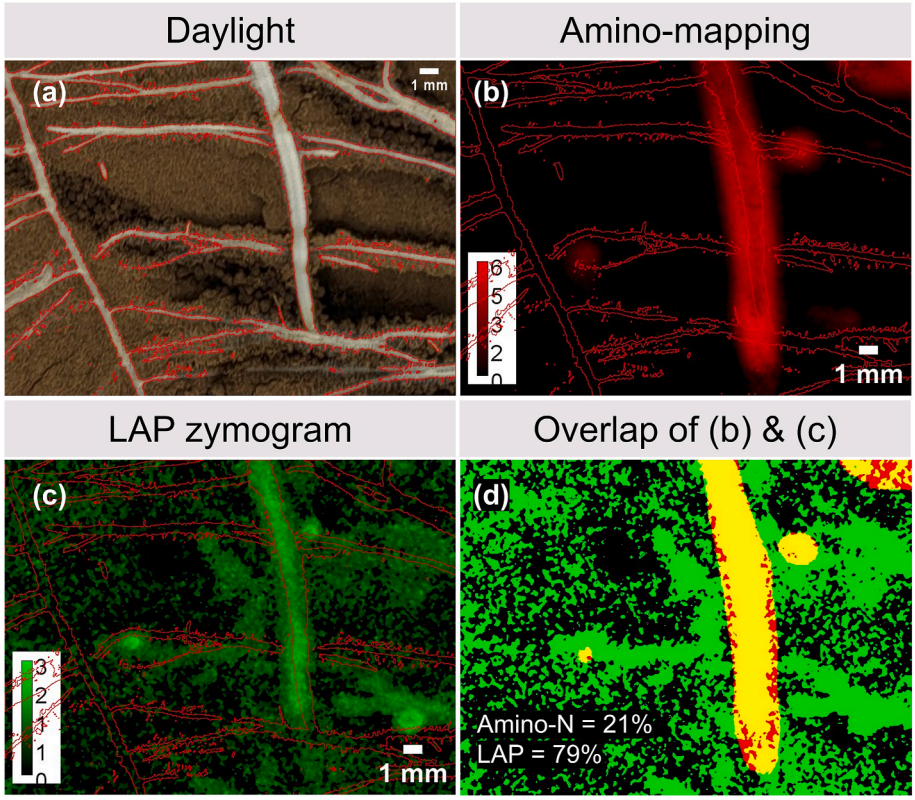

Fig. 5. Example of amino-N content and leucine aminopeptidase (LAP) activity co-localization in seminal roots. (a) Daylight image of soil-root surface with red lines highlight the root boundary. (b) Amino-N distribution is illustrated with a red bar indicating the amino-N content (ng mm^{-2}). (c) LAP activity distribution is illustrated with green bar indicating the LAP activity (pmol mm^{-2} min^{-1}). (d) The yellow overlap image represents the co-localization of amino-N (red) and LAP activity (green). Co-localization analysis is presented via two coefficients: Amino-N (21% of the LAP area overlaps with amino-N) and LAP (79% of the amino-N area overlaps with LAP).

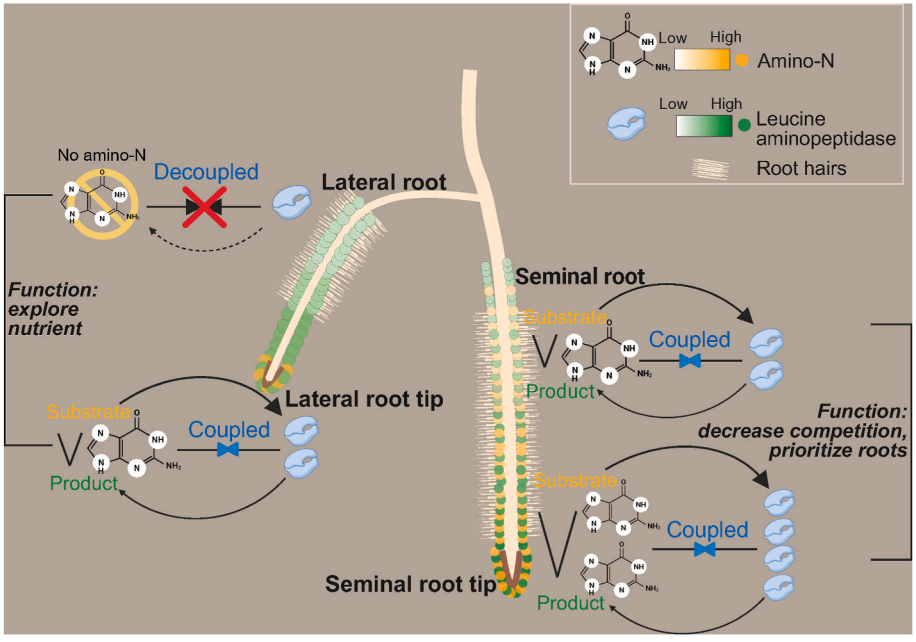

Fig. 6. Conceptual diagram represents the relationship between amino-N and leucine aminopeptidase activity across different root parts. Yellow circles around root indicate amino-N content, green circles around root indicate leucine aminopeptidase activity, color density indicates the level of activity. The role of seminal roots and their tips is to alleviate the competition for nutrients between roots and microorganisms, emphasizing the priority needs of the roots. In contrast, lateral roots are predominately responsible for exploring soil nutrients, with the help of microbial community to fulfil their nutritional requirements.

suggest potential N limitation. Another possible explanation for the absence of detectable amino-N could be the rapid uptake and assimilation by microorganisms, which could limit its accumulation. In bulk soil, the secondary substrates from re-utilization of microbial residues could play a larger role, with smaller amounts and a rapid rate of consumption of organic N as compared to the rhizosphere. The turnover of organic substrates could mainly occur inside the soil pores rather than on the aggregate surfaces. This could explain negligible amino-N content detected in the soil by our visualization approach.

Further research should integrate information on the expression of functional genes related to amino-N production and the enzymes that release amino-N to investigate their relationship. It is also crucial to integrate the functions of different root parts into a general concept. Among these, particular emphasis should be placed on the lateral root tips, as they have the highest potential to drive nutrient cycling in the rhizosphere. While this study provides valuable insights into the spatial distribution of amino-N and LAP activity in the rhizosphere, some limitations should be considered. The composition and origin of the amino-N we measured remains uncertain, mainly due to relatively large amount of sample (in comparison to very small soil volume surrounding individual parts of the root) required to integrate advanced techniques such as gas chromatography-mass spectrometry to identify and quantify specific amino-N compounds. Another limitation is that the analytical method used may be more suited for detecting amino-N on the roots with less sensitivity in the surrounding soil. Finally, our study focused on a specific plant species and environmental conditions, and further research could explore whether similar patterns are observed in other crops and how environmental factors such soil type, microbial community composition, and plant developmental stage influence the processes of organic N transformation in the rhizosphere to enhance the applicability of the findings for N management in agricultural systems.

5. Conclusions

Development of the local thresholding approach LZDT enabled to better quantify the spatial distributions of amino-N content and LAP activity in the rhizosphere of different root parts of *Zea mays* L. Our findings revealed an inhomogeneous spatial distribution of amino-N content, with significant allocation to newly developing segments. However, specific locations, such as lateral roots and root-free soil, did not show visible amino-N content, despite the detection of relatively high enzymatic activity. The combination of amino-mapping and leucine aminopeptidase (LAP) activity zymography revealed the relationship between amino-N content and LAP activity distribution in various root segments at the soil-root interface. Amino-N content and LAP activity were co-localized and positively correlated with each other, although this relationship depended on specific root parts. The highest amino-N content and LAP activity were observed in the seminal root tips, whereas the relative rhizosphere extent of amino-N content and LAP activity was greatest at lateral root tips, emphasizing the dynamic and localized nature of nutrient cycling processes. This study provides insights into the close relationship between N distribution and enzymatic activity in the rhizosphere, contributing to the functional heterogeneity of different root zones. It also underscores the importance of considering the specificity of different root parts when analyzing these dynamics. Such functional heterogeneity and specificity of different root parts needs to be considered in the strategies to improve nutrient use efficiency in agricultural systems.

CRediT authorship contribution statement

Guoting Shen: Writing – original draft, Visualization, Investigation, Conceptualization. **Andrey Guber:** Writing – review & editing, Visualization, Software, Methodology, Funding acquisition. **Sajedeh Khosrozadeh:** Writing – review & editing, Methodology. **Negar Ghaderi:** Writing – review & editing, Methodology. **Alexandra Kravchenko:** Writing – review & editing, Visualization, Software, Methodology. **Evgenia Blagodatskaya:** Writing – review & editing, Supervision, Methodology, Funding acquisition, Conceptualization.

Declaration of competing interest

The authors declare that they have no known competing financial interests or personal relationship that could have appeared to influence the work reported in this paper.

Acknowledgements

The authors gratefully acknowledge the China Scholarship Council (CSC) for financial support to GS. This work was conducted within the framework of the priority program 2089, funded by the Deutsche Forschungsgemeinschaft (DFG, German Research Foundation) – Project number: 403664478. Seeds of the maize were provided by Caroline Marcon and Frank Hochholdinger (University of Bonn). Support for this research was provided by the Great Lakes Bioenergy Research Center, U. S. Department of Energy, Office of Science, Office of Biological and Environmental Research (Award DE-SC0018409), by the National Science Foundation Long-term Ecological Research Program (DEB 2224712) at the Kellogg Biological Station, and by USDA-NIFA, Award no. 2022-67019-36104.

Appendix A. Supplementary data

Supplementary data to this article can be found online at https://doi.org/10.1016/j.rhisph.2025.101024.

Data availability

Data will be made available on request.

References

Amicucci, M.J., Galermo, A.G., Guerrero, A., Treves, G., Nandita, E., Kailemia, M.J., Higdon, S.M., Pozzo, T., Labavitch, J.M., Bennett, A.B., Lebrilla, C.B., 2019. Strategy for structural elucidation of polysaccharides: elucidation of a maize mucilage that harbors diazotrophic bacteria. Anal. Chem. 91, 7254–7265.

Bais, H.P., Weir, T.L., Perry, L.G., Gilroy, S., Vivanco, J.M., 2006. The role of root exudates in rhizosphere interations with plants and other organisms. Annu. Rev. Plant Biol. 57, 233–266.

Bates, D., Mächler, M., Bolker, B., Walker, S., 2015. Fitting linear mixed-effects models using lme4. J. Stat. Software 67, 1–48.

Bilyera, N., Kuzyakova, I., Guber, A., Razavi, B.S., Kuzyakov, Y., 2020. How "hot" are hotspots: statistically localizing the high-activity areas on soil and rhizosphere images. Rhizosphere 16, 100259.

Bilyera, N., Zhang, X., Duddek, P., Fan, L., Banfield, C.C., Schlüter, S., Carminati, A., Kaestner, A., Ahmed, M.A., Kuzyakov, Y., Dippold, M.A., Spielvogel, S., Razavi, B.S., 2021. Maize genotype-specific exudation strategies: an adaptive mechanism to increase microbial activity in the rhizosphere. Soil Biol. Biochem. 162, 108426.

Canarini, A., Kaiser, C., Merchant, A., Richter, A., Wanek, W., 2019. Root exudation of primary metabolites: mechanisms and their roles in plant responses to environmental stimuli. Front. Plant Sci. 10, 157.

Darwent, M.J., Paterson, E., McDonald, A.J.S., Tomos, A.D., 2003. Biosensor reporting of root exudation from *Hordeum vulgare* in relation to shoot nitrate concentration. J. Exp. Bot. 54, 325–334.

Dupuy, L.X., Silk, W.K., 2016. Mechanisms of early microbial establishment on growing root surfaces. Vadose Zone J. 15, 1–13.

Fierer, N., Bradford, M.A., Jackson, R.B., 2007. Toward an ecological classification of soil bacteria. Ecology 88, 1354–1364.

Geisseler, D., Horwath, W.R., 2014. Investigating amino acid utilization by soil microorganisms using compound specific stable isotope analysis. Soil Biol. Biochem. 74, 100–105.

Geisseler, D., Horwath, W.R., Joergensen, R.G., Ludwig, B., 2010. Pathways of nitrogen utilization by soil microorganisms - a review. Soil Biol. Biochem. 42, 2058–2067.

Ghaderi, N., Schmidt, H., Schlüter, S., Banfield, C., Blagodatskaya, E., 2022. Development of micro-zymography: visualization of enzymatic activity at the microscopic scale for aggregates collected from the rhizosphere. Plant Soil 478, 253–271.

Greenfield, L.M., Hill, P.W., Paterson, E., Baggs, E.M., Jones, D.L., 2020. Do plants use root-derived proteases to promote the uptake of soil organic nitrogen? Plant Soil 456, 355–367.

Greenfield, L.M., Razavi, B.S., Bilyera, N., Zhang, X., Jones, D.L., 2021. Root hairs and protein addition to soil promote leucine aminopeptidase activity of *Hordeum vulgare* L. Rhizosphere 18, 100329.
Guber, A., Blagodatskaya, E., Juyal, A., Razavi, B.S., Kuzyakov, Y., Kravchenko, A., 2021. Time-lapse approach to correct deficiencies of 2D soil zymography. Soil Biol. Biochem. 157, 108225.
Guber, A., Kraychenko, A., Razavi, B.S., Uteau, D., Peth, S., Blagodatskaya, E., Kuzyakov, Y., 2018. Quantitative soil zymography: mechanisms, processes of substrate and enzyme diffusion in porous media. Soil Biol. Biochem. 127, 156–167.
Hao, C., Dungait, J.A.J., Wei, X., Ge, T., Kuzyakov, Y., Cui, Z., Tian, J., Zhang, F., 2022. Maize root exudate composition alters rhizosphere bacterial community to control hotspots of hydrolase activity in response to nitrogen supply. Soil Biol. Biochem. 170, 108717.
Hartman, K., Tringe, S.G., 2019. Interactions between plants and soil shaping the root microbiome under abiotic stress. Biochem. J. 476, 2705–2724.
Hartmann, A., Schmid, M., van Tuinen, D., Berg, G., 2009. Plant-driven selection of microbes. Plant Soil 321, 235–257.
Heitkötter, J., Marschner, B., 2018. Soil zymography as a powerful tool for exploring hotspots and substrate limitation in undisturbed subsoil. Soil Biol. Biochem. 124, 210–217.
Hill, E.J., Jones, D.L., Paterson, E., Hill, P.W., 2019. Hotspots and hot moments of amino acid N in soil: real-time insights using continuous microdialysis sampling. Soil Biol. Biochem. 131, 40–43.
Holz, M., Zarebanadkouki, M., Kuzyakov, Y., Pausch, J., Carminati, A., 2018. Root hairs increase rhizosphere extension and carbon input to soil. Ann. Bot. 121, 61–69.
Houlden, A., Timms-Wilson, T.M., Day, M.J., Bailey, M.J., 2008. Influence of plant developmental stage on microbial community structure and activity in the rhizosphere of three field crops. FEMS Microbiol. Ecol. 65, 193–201.
Jian, S., Li, J., Chen, J., Wang, G., Mayes, M.A., Dzantor, K.E., Hui, D., Luo, Y., 2016. Soil extracellular enzyme activities, soil carbon and nitrogen storage under nitrogen fertilization: a meta-analysis. Soil Biol. Biochem. 101, 32–43.
Jones, D.L., Darrah, P.R., 1994. Amino-acid influx at the soil-root interface of *Zea mays* L. and its implications in the rhizosphere. Plant Soil 163, 1–12.
Jones, D.L., Owen, A.G., Farrar, J.F., 2002. Simple method to enable the high resolution determination of total free amino acids in soil solutions and soil extracts. Soil Biol. Biochem. 34, 1893–1902.
Khosrozadeh, S., Guber, A., Kravchenko, A., Ghaderi, N., Blagodatskaya, E., 2022. Soil oxidoreductase zymography: visualizing spatial distributions of peroxidase and phenol oxidase activities at the root-soil interface. Soil Biol. Biochem. 167, 108610.
Khosrozadeh, S., Guber, A., Nourbakhsh, F., Khalili, B., Blagodatskaya, E., 2023. Amino mapping: possibility to visualize amino-N compounds in the rhizosphere of *Zea Mays* L. Biol. Fertil. Soils 59, 1007–1011.
Kuzyakov, Y., Xu, X.L., 2013. Competition between roots and microorganisms for nitrogen: mechanisms and ecological relevance. New Phytol. 198, 656–669.
Leduc, S.D., Rothstein, D.E., 2010. Plant-available organic and mineral nitrogen shift in dominance with forest stand age. Ecology 91, 708–720.
Li, X.Z., Rui, J.P., Mao, Y.J., Yannarell, A., Mackie, R., 2014. Dynamics of the bacterial community structure in the rhizosphere of a maize cultivar. Soil Biol. Biochem. 68, 392–401.
Lipson, D., Näsholm, T., 2001. The unexpected versatility of plants: organic nitrogen use and availability in terrestrial ecosystems. Oecologia 128, 305–316.
Ma, X., Razavi, B.S., Holz, M., Blagodatskaya, E., Kuzyakov, Y., 2017. Warming increases hotspot areas of enzyme activity and shortens the duration of hot moments in the root-detritusphere. Soil Biol. Biochem. 107, 226–233.
Ma, X.M., Zarebanadkouki, M., Kuzyakov, Y., Blagodatskaya, E., Pausch, J., Razavi, B.S., 2018. Spatial patterns of enzyme activities in the rhizosphere: effects of root hairs and root radius. Soil Biol. Biochem. 118, 69–78.
Matsui, M., Fowler, J.H., Walling, L.L., 2006. Leucine aminopeptidases: diversity in structure and function. Biol. Chem. 387, 1535–1544.
McCormack, M.L., Dickie, I.A., Eissenstat, D.M., Fahey, T.J., Fernandez, C.W., Guo, D.L., Helmisaari, H.S., Hobbie, E.A., Iversen, C.M., Jackson, R.B., Leppalammi-Kujansuu, J., Norby, R.J., Phillips, R.P., Pregitzer, K.S., Pritchard, S.G., Rewald, B., Zadworny, M., 2015. Redefining fine roots improves understanding of below-ground contributions to terrestrial biosphere processes. New Phytol. 207, 505–518.
Meier, I.C., Tückmantel, T., Heitkötter, J., Müller, K., Preusser, S., Wrobel, T.J., Kandeler, E., Marschner, B., Leuschner, C., 2020. Root exudation of mature beech forests across a nutrient availability gradient: the role of root morphology and fungal activity. New Phytol. 226, 583–594.
Neumann, G., Römheld, V., 2011. Rhizosphere chemistry in relation to plant nutrition. In: Marschner's Mineral Nutrition of Higher Plants. Academic press, Amsterdam.
Pausch, J., Kuzyakov, Y., 2011. Photoassimilate allocation and dynamics of hotspots in roots visualized by ^{14}C phosphor imaging. J. Plant Nutr. Soil Sci. 174, 12–19.
Perkins, A.C., Lynch, J.P., 2021. Increased seminal root number associated with domestication improves nitrogen and phosphorus acquisition in maize seedlings. Ann. Bot. 128, 453–468.
Postma, J.A., Dathe, A., Lynch, J.P., 2014. The optimal lateral root branching density for maize depends on nitrogen and phosphorus availability. Plant Physiol. 166, 590–602.
Razavi, B.S., Zarebanadkouki, M., Blagodatskaya, E., Kuzyakov, Y., 2016. Rhizosphere shape of lentil and maize: spatial distribution of enzyme activities. Soil Biol. Biochem. 96, 229–237.
Rogers, E.D., Benfey, P.N., 2015. Regulation of plant root system architecture: implications for crop advancement. Curr. Opin. Biotechnol. 32, 93–98.
Rohde, F., Braumann, U.-D., Schmidt, M., 2020. *Correlia*: an *ImageJ* plug-in to co-register and visualise multimodal correlative micrographs. J. Microsc. 280, 3–11.
Rüger, L., Feng, K., Dumack, K., Freudenthal, J., Chen, Y., Sun, R., Wilson, M., Yu, P., Sun, B., Deng, Y., Hochholdinger, F., Vetterlein, D., Bonkowski, M., 2021. Assembly patterns of the rhizosphere microbiome along the longitudinal root Axis of maize (*Zea mays* L.). Front. Microbiol. 12, 614501.
Sinsabaugh, R.L., Follstad Shah, J.J., 2011. Ecoenzymatic stoichiometry of recalcitrant organic matter decomposition: the growth rate hypothesis in reverse. Biogeochemistry 102, 31–43.
Sinsabaugh, R.L., Lauber, C.L., Weintraub, M.N., Ahmed, B., Allison, S.D., Crenshaw, C., Contosta, A.R., Cusack, D., Frey, S., Gallo, M.E., Gartner, T.B., Hobbie, S.E., Holland, K., Keeler, B.L., Powers, J.S., Stursova, M., Takacs-Vesbach, C., Waldrop, M. P., Wallenstein, M.D., Zak, D.R., Zeglin, L.H., 2008. Stoichiometry of soil enzyme activity at global scale. Ecol. Lett. 11, 1252–1264.
Tai, H.H., Lu, X., Opitz, N., Marcon, C., Paschold, A., Lithio, A., Nettleton, D., Hochholdinger, F., 2016. Transcriptomic and anatomical complexity of primary, seminal, and crown roots highlight root type-specific functional diversity in maize (*Zea mays* L.). J. Exp. Bot. 67, 1123–1135.
Vetterlein, D., Doussan, C., 2016. Root age distribution: how does it matter in plant processes? A focus on water uptake. Plant Soil 407, 145–160.
Vetterlein, D., Lippold, E., Schreiter, S., Phalempin, M., Fahrenkampf, T., Hochholdinger, F., Marcon, C., Tarkka, M., Oburger, E., Ahmed, M., Javaux, M., Schluter, S., 2021. Experimental platforms for the investigation of spatiotemporal patterns in the rhizosphere-laboratory and field scale. J. Plant Nutr. Soil Sci. 184, 35–50.
Vitousek, P.M., Hattenschwiler, S., Olander, L., Allison, S., 2002. Nitrogen and nature. Ambio 31, 97–101.
Wei, T., Simko, V., Levy, M., Xie, Y., Jin, Y., Zemla, J., 2017. Package 'corrplot'. Statistician 56, e24.
Wichern, F., Eberhardt, E., Mayer, J., Joergensen, R.G., Muller, T., 2008. Nitrogen rhizodeposition in agricultural crops: methods, estimates and future prospects. Soil Biol. Biochem. 40, 30–48.
Williams, A., Langridge, H., Straathof, A.L., Muhamadali, H., Hollywood, K.A., Goodacre, R., de Vries, F.T., 2022. Root functional traits explain root exudation rate and composition across a range of grassland species. J. Ecol. 110, 21–33.
Yu, P., Baldauf, J.A., Lithio, A., Marcon, C., Nettleton, D., Li, C.J., Hochholdinger, F., 2016. Root type-specific reprogramming of maize pericycle transcriptomes by local high nitrate results in disparate lateral root branching patterns. Plant Physiol. 170, 1783–1798.
Yu, P., He, X., Baer, M., Beirinckx, S., Tian, T., Moya, Y.A., Zhang, X., Deichmann, M., Frey, F.P., Bresgen, V., 2021. Plant flavones enrich rhizosphere Oxalobacteraceae to improve maize performance under nitrogen deprivation. Nat. Plants 7, 481–499.
Zhan, A., Lynch, J.P., 2015. Reduced frequency of lateral root branching improves N capture from low-N soils in maize. J. Exp. Bot. 66, 2055–2065.